JOURNAL OF Materials CHEMISTRY

The synthesis, structure and properties of $Hg_2Os_2O_7$

Jonathan Reading,[a] Sergey Gordeev[b] and Mark T. Weller[a]

[a]*Department of Chemistry, University of Southampton, Southampton, Hants, UK SO17 1BJ. E-mail: mtw@soton.ac.uk*
[b]*Department of Physics, University of Southampton, Southampton, Hants, UK SO17 1BJ*

Received 24th October 2001, Accepted 14th November 2001
First published as an Advance Article on the web 16th January 2002

$Hg_2Os_2O_7$ has been synthesised by direct reaction of HgO, OsO_4 and Os metal at 500 °C. The product adopts the pyrochlore structure, in common with $Cd_2Os_2O_7$, but exhibits a slightly larger lattice parameter at 10.245 Å. The material shows a weak transition to antiferromagnetic behaviour below 88 K; the compound remains semi-metallic through this transition but with a distinct drop in resistivity again centred on 88 K. Powder neutron diffraction data, collected over the temperature range 12 K–298 K, show weak discontinuities in the structural properties at this transition. Comparisons are made with the $Cd_2Os_2O_7$ and $Cd_2Re_2O_7$ systems.

Introduction

The pyrochlore structure is commonly adopted by materials of the composition $A_2M_2O_{7-x}$ where A is a larger mono-, di- or tri-valent cation and M is a smaller tetra-, penta- or hexa-valent cation. Examples include $Mn_2Sb_2O_7$, $Sn_2Ta_2O_7$ and $Pb_2U_2O_7$. The structure can be drawn using MO_6 octahedra sharing all vertices with a distorted (6 + 2) cubic co-ordination to the A type cation, Fig. 1. Alternatively the structure can be considered as being derived from a fluorite structure with the composition $[A_2M_2]O_8$ by the removal of two oxide anions in a regular fashion producing, $A_2M_2O_7\square$, where $\square$ represents a vacancy. A detailed review of the pyrochlore system describing the wealth of materials adopting this structure type and their properties has been published by Subramanian and co-workers.[1] Recently much work on pyrochlore chemistry has been directed at the magnetic and electronic properties of materials in this system that contain late second row transition elements as the M type cation. For example, the ruthenium(IV) pyrochlores such as $Ln_2Ru_2O_7$ and $Y_2Ru_2O_7$ have been investigated in terms of their magnetic structures and magnetic frustration by a number of groups.[2–4] Further attention has focussed on $Tl_2Ru_2O_7$ which exhibits strong magnetoresistive effects.[5,6]

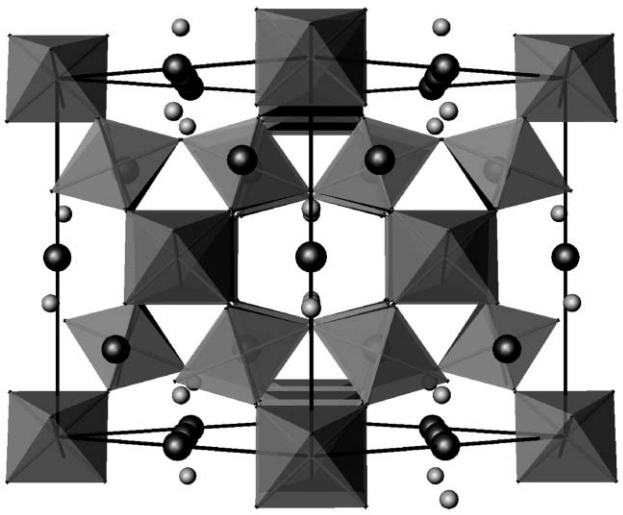

Fig. 1 The pyrochlore structure, viewed down 110, formed from BO_6 octahedra, A cations (large darker spheres) and O′ oxygen (small paler spheres).

One of the pyrochlores originally reported by Sleight[7] as part of a systematic study of materials with this structure type in the early 1970s was the more unusual (2+, 5+) material $Cd_2Os_2O_7$. This compound was found to exhibit an electronic second order metal to semiconductor/insulator transition at 225 K, T_{MI}, with an associated antiferromagnetic ordering. We have recently reported a detailed structural investigation of this material through its transition at 225 K and observed systematic changes in structural parameters either side of the transition temperature consistent with the change for semi-conducting to metallic properties.[8] No evidence was found of long range magnetic ordering below 225 K in the neutron scattering experiments presumably because the magnetic moments are frustrated. However, the expected weak magnetic scattering and rapid drop off of magnetic form factors for third row transition metals might mitigate against observing magnetic reflections. The electronic and magnetic properties of this material have also been recently reported in great detail by Mandrus *et al*[9] who describe the transformation at 225 K as the first well-documented example of a pure Slater transition. Further recent interest in cadmium containing pyrochlores is evidenced by the report of superconductivity, for the first time in a pyrochlore structure, in $Cd_2Re_2O_7$ below 1.1 K[10] and studies of the electronic structure of this and the cadmium osmate.[11]

$Ca_{2-y}Os_2O_{7-x}$ has also been reported as a pyrochlore type phase by a number of authors.[12–14] Cubic, tetragonal and orthorhombic forms of this compound have been described with the product structure depending upon the synthesis method used and the product composition. This material is also reported as having a metal–insulator transition near room temperature or as being metallic, again depending on compound composition.

The observation of osmium(V) in complex oxides is extremely rare and previous to the recent work on $Cd_2Os_2O_7$ only one other Os(V) complex oxide has had its structure reported, namely $NdOsO_4$,[15] which also has a structure based on linked OsO_6 octahedra. In their review article Subramiam *et al*[1] summarised the known (2+,5+) pyrochlores oxides for late transition metals in terms of their ionic radii. From these considerations based on cation sizes it is clear that many Hg(II) based pyrochlores should exist with this ion in combination with a variety of pentavalent species. Of these compositions only $Hg_2B_2O_7$ with B = Nb, Ta and Sb and $Hg_2V_2O_7$ have

 DOI: 10.1039/b109715f

been synthesised and characterised presumably in part due to problems in reacting HgO without decomposition. In this article we report the synthesis of $Hg_2Os_2O_7$, a full structural study of this material between 12 K and room temperature and preliminary investigations of its electronic and magnetic properties.

Experimental

Samples of $Hg_2Os_2O_7$ were prepared by grinding together high purity stoichiometric mixtures of HgO (99.8%), Os (99.8%) and OsO_4 (99.95%). The mixture was loaded into a silica ampoule and sealed under vacuum with the sample end immersed in liquid nitrogen to avoid osmium loss due to the volatility of OsO_4. The mixture was heated at 500 °C for 1 day then furnace cooled to room temperature. **Caution**: heating the tube to higher temperatures can lead to disintegration of the tube and loss of mercury as the metal vapour. Powder X-ray diffraction data were recorded on the black product using a Siemens D5000 diffractometer operating with $CuK_{\alpha 1}$ radiation. The pattern was consistent with phase pure pyrochlore product material, with a cubic unit cell of dimension $a = 10.245$ Å.

Powder neutron diffraction

Time of flight (TOF) powder neutron diffraction data were collected on the GEM and POLARIS diffractometers at the Rutherford Appleton Laboratory, Oxfordshire, UK. The experiment was carried out using a closed cycle refrigeration (CCR) system at a series of temperatures, ranging from 12 K to room temperature. Data were collected for periods between 60 and 135 minutes at each temperature; the shorter times being used for the higher flux GEM instrument. The room temperature data set was collected initially followed by cooling to 12 K and staged heating back to 50 K (POLARIS) or cooling to 70 K and staged heating back to RT (GEM). The lower temperature data were collected on POLARIS due to problems in reaching and maintaining temperature stability using existing cryoloop equipment on GEM. No additional reflection was observed in the data collected at the lowest temperatures indicating that no long range magnetic ordering occurs in this material.

Rietveld refinement of structure was undertaken using GSAS[16] and used the cubic pyrochlore model in the space group $Fd\bar{3}m$ together with the accepted neutron scattering lengths.[17] For the structure refinements using the POLARIS data only the back-scattering bank was used, for the GEM data all four banks were used. A uniform approach to the structure refinement was undertaken for each of the data sets obtained at different temperatures to ensure consistent results. Cell parameters, peak shape parameters atomic positions and isotropic temperature factors were sequentially added to the refinement. No evidence of fractional site occupancies was observed. For each data set the refinement converged smoothly; Fig. 2 shows the (typical) fit obtained to the room temperature data from GEM. Derived lattice parameters, atomic co-ordinates, displacement factors ($100U_{eq}/Å^2$) and profile fit parameters at each temperature are summarised in Table 1 together with the crystallographic description of the structure. Fit parameters and χ^2 values show behaviour in line with the data collection times.

Magnetic and electronic measurements

Magnetic susceptibility data were collected on a 100 mg sample using a VSM over the temperature range 4 K to room temperature. Electronic resistivity data were obtained using a typical four probe apparatus on a 10 mm × 4 mm × 1 mm bar

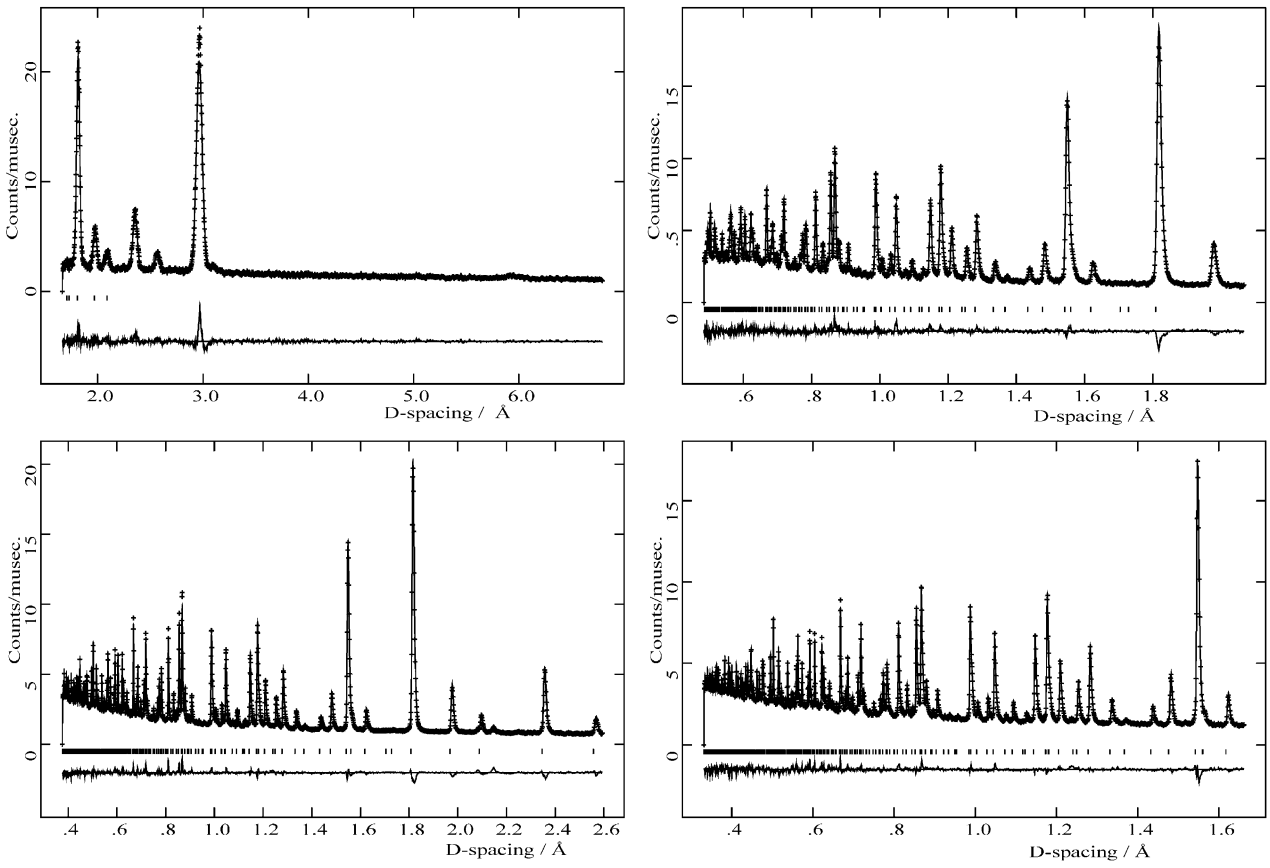

Fig. 2 Fits obtained to the powder neutron diffraction data obtained from $Hg_2Os_2O_7$ on GEM. Data from the four data banks used, at 18, 64, 91 and 154°, in terms of *d*-spacing are shown from top left to bottom right.

Table 1 Summary of derived atomic, thermal and profile fit parameters for $Hg_2Os_2O_7$ as a function of temperature; esds are given in parentheses. Space group $Fd\bar{3}m$. Hg on (½,½,½), Os on (0,0,0), O1 on $(x,\frac{1}{8},\frac{1}{8})$ O2 on $(\frac{3}{8},\frac{3}{8},\frac{3}{8})$

T/K	a/Å	O1 x	Hg U_{iso} × 100 Å^2	Os U_{iso} × 100 Å^2	O1 U_{iso} × 100 Å^2	O2 U_{iso} × 100 Å^2	R_{wp} (%)	R_p (%)	χ^2
12[a]	10.23469(3)	0.31736(6)	0.111(5)	0.112(6)	0.382(6)	0.38(2)	1.98	5.18	2.56
25[a]	10.23486(3)	0.31729(6)	0.118(6)	0.139(7)	0.387(6)	0.43(2)	2.50	7.44	1.44
50[a]	10.23519(3)	0.31731(6)	0.157(6)	0.129(7)	0.394(6)	0.43(2)	2.38	7.49	1.32
70	10.23563(3)	0.31736(6)	0.078(6)	0.003(6)	0.264(6)	0.35(2)	4.39	3.63	4.54
75	10.23580(3)	0.31731(6)	0.095(6)	0.008(6)	0.271(6)	0.38(2)	4.31	3.58	4.37
80	10.23592(3)	0.31727(6)	0.107(6)	0.008(6)	0.282(6)	0.38(2)	4.32	3.66	4.41
85	10.23608(3)	0.31735(6)	0.109(6)	0.014(6)	0.277(6)	0.39(2)	4.24	3.59	4.23
90	10.23615(3)	0.31736(6)	0.115(6)	0.016(6)	0.281(6)	0.39(2)	4.28	3.57	4.31
95	10.23629(3)	0.31725(6)	0.115(6)	0.013(6)	0.279(6)	0.39(2)	4.25	3.56	4.24
100	10.23640(3)	0.31727(6)	0.124(6)	0.016(7)	0.286(6)	0.40(2)	4.29	3.62	4.35
110	10.23658(3)	0.31727(6)	0.125(6)	0.025(6)	0.297(6)	0.40(2)	4.21	3.59	4.16
130	10.23701(3)	0.31731(6)	0.141(6)	0.026(6)	0.298(6)	0.42(2)	4.20	3.55	4.14
160	10.23790(3)	0.31710(6)	0.176(7)	0.037(7)	0.318(6)	0.46(2)	4.16	3.50	4.10
200	10.23961(3)	0.31710(5)	0.232(7)	0.063(7)	0.367(6)	0.55(2)	4.06	3.46	3.91
250	10.24258(3)	0.31701(7)	0.320(8)	0.102(7)	0.434(6)	0.68(2)	3.86	3.31	3.54
300	10.24681(3)	0.31686(7)	0.429(9)	0.142(8)	0.524(6)	0.81(2)	3.83	3.36	3.53

[a]POLARIS data.

of polycrystalline $Hg_2Os_2O_7$ pressed under 10 tonnes cm^{-2} coated with silver paint to make good contact.

Results

Reaction of HgO, OsO_4 and Os metal at 500 °C results in the rapid formation of pure $Hg_2Os_2O_7$ as a black shiny solid. The material adopts the cubic pyrochlore structure with $a \sim 10.245$ Å at room temperature. The reaction temperature required for formation of the mercury osmate is rather lower than that required for the cadmium analogue presumably due the increased reactivity and volatility of HgO compared with CdO. Attempts to produce $Hg_2Os_2O_7$ under the same conditions as $Cd_2Os_2O_7$ were unsuccessful leading to decomposition to mercury metal. Similarly attempts to produce phases in the solid solution $(Hg_{1-x}Cd_x)_2Os_2O_7$ produced mixed phase material containing the ternary pyrochlore end members or $Hg_2Os_2O_7$ plus CdO and OsO_2.

Magnetic and electronic properties

The magnetic susceptibility of $Hg_2Os_2O_7$ between 4 K and 298 K is shown in Fig. 3. A broad cusp is centred on 88 K is apparent showing formation of a weakly antiferromagnetic structure. The shape and dimensions of the curve are similar to that observed for $Cd_2Os_2O_7$.[7,9]

Resistivity data are shown in Fig. 4. The upper data set was obtained from the sample cooled in zero magnetic field while the lower trace, obtained on heating, was obtained in a magnetic field of 5 T. The absolute value near 0.0025 mΩ cm is typical of a poor metal and only changes very weakly with temperature. A small, but marked decrease, centred on 88 K, is apparent but this change is much weaker than the orders of magnitude change observed at 225 K for single crystals of $Cd_2Os_2O_7$ and is in the opposite direction. A very small magnetoresistive effect was also discernible. The absolute values are similar to those found for $Cd_2Re_2O_7$[11] but there is no sign of superconductivity above 4 K and we were unable to cool the sample below this temperature using our apparatus. Similar electronic behaviour has also been observed for $Cd_2Ru_2O_7$[18] and interpreted in terms of the stabilisation of a spin-density wave at 100 K in this material.

Structure

The variation of the lattice parameter of $Hg_2Os_2O_7$ between 12 K and room temperature is shown in Fig. 5. Normal expansion of a complex oxide would generally result in a close to linear increase in cell parameter as a function of temperature with a less rapid decrease as the sample temperature approaches 0 K. The data show somewhat anomalous behaviour at around 85–90 K, Fig. 5 inset, which show almost no increase in lattice parameter between these temperatures. Below 80 K and between 90 K and 200 K the lattice parameter increases approximately linearly at around 1.5×10^{-5} Å K^{-1}. The very small inflection seen between 85 K

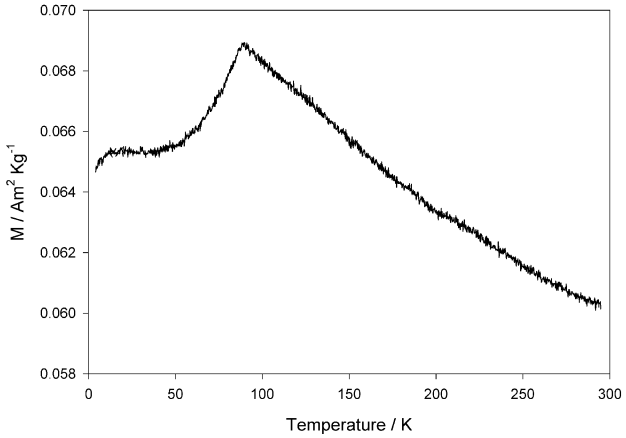

Fig. 3 The temperature dependence of the magnetic susceptibility for $Hg_2Os_2O_7$.

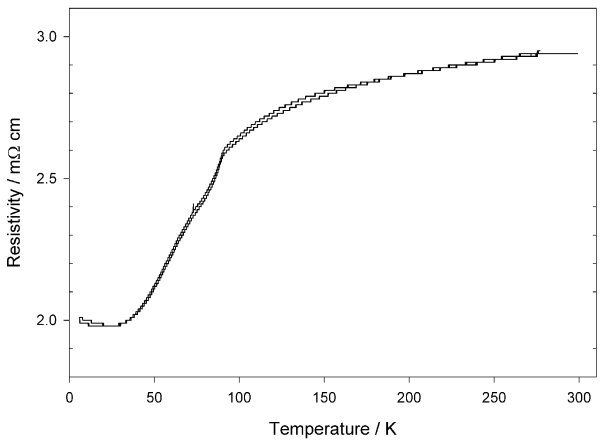

Fig. 4 The temperature dependence of the resistivity for $Hg_2Os_2O_7$.

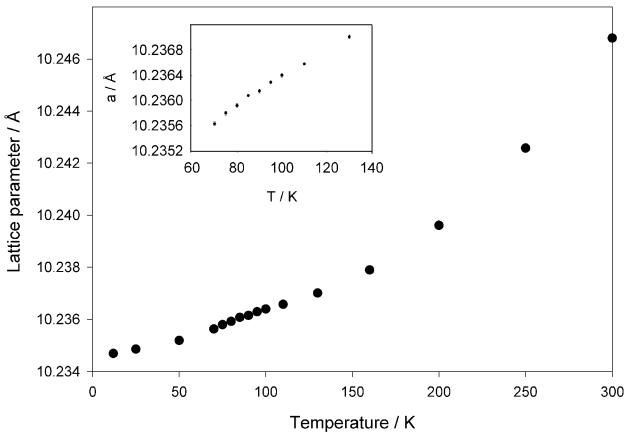

Fig. 5 The variation of the lattice parameter of $Hg_2Os_2O_7$ as a function of temperature between 12 and 298 K. The inset expands the region between 70 and 130 K. Error bars are shown but in the main graph are within the plotted symbol dimensions.

and 90 K might be associated with the weak antiferromagnetic transition observed at 88 K.

In terms of the structural parameters only one position is refinable in the pyrochlore structural model, the O1 x co-ordinate; for a value of 0.3125 this produces perfect MO_6 octahedra. The refined value in $Hg_2Os_2O_7$ is around 0.317 which represents a small trigonal distortion of this unit producing bond angles around osmium of approximately 91.9° (×3) and 88.1° (×3). The variation of this oxygen co-ordinate as a function of temperature is plotted in Fig. 6 and shows steady value up to around 130 K before a significant decrease with increasing temperature. Coupling the change in this oxygen position with the increasing lattice parameter produces the variations in Os–O bond length in the OsO_6 octahedron seen in Fig. 7 and the internal O–Os–O octahedral angle shown in Fig. 8. The normal behaviour of structures built from MO_6 octahedra would be a smooth increase in metal–oxygen bond lengths as the structure expands associated with the formation of more regular octahedra. The data here is abnormal in terms of totally static behaviour below 130 K before the structural parameters show the normal manifestations of expansion. At the same time the inter OsO_6 octahedra angles become more regular as shown in Fig. 9 and the Hg–O distances increase, Fig. 10. The Os–O bond length is similar to that found in $Cd_2Os_2O_7$ [8] consistent with the description of this material as containing Os(v).

The variations of the individual thermal parameters are shown in Fig. 11. As the data from the lowest three

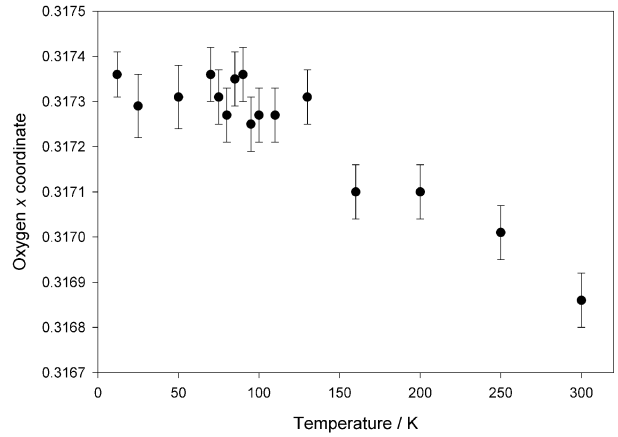

Fig. 6 The variation of the O1 x co-ordinate between 12 and 298 K.

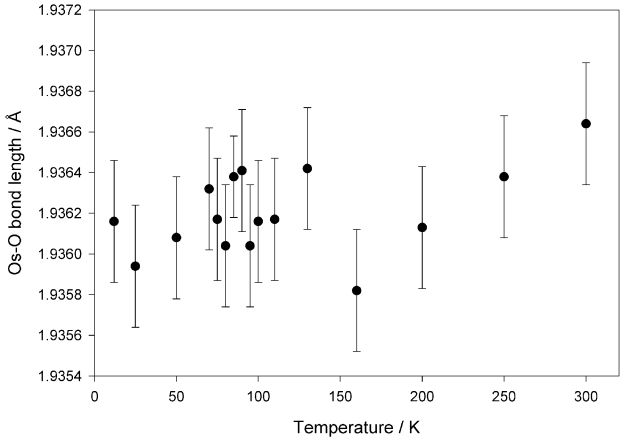

Fig. 7 The variation of the Os–O bond length between 12 and 298 K.

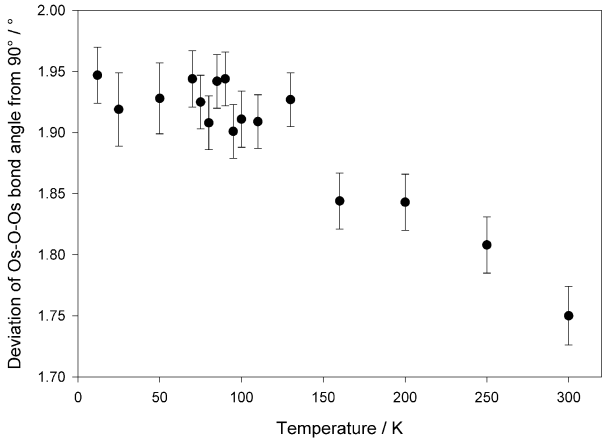

Fig. 8 The variation of the distortion of the O–Os–O from 90° between 12 and 298 K.

temperatures, 12, 25 and 50 K, were collected on POLARIS they are not shown on these graphs; due to the different instrument parameters, sample size and mounting small differences are expected in such parameters from different instruments. The data from POLARIS show similar trends to that from GEM, as shown in Table 1, but displaced to higher U_{eq} values by typically 0.0012 Å^2. For each atom the variation of thermal displacement parameters shows similar behaviour with the expected increase with temperature; some evidence is

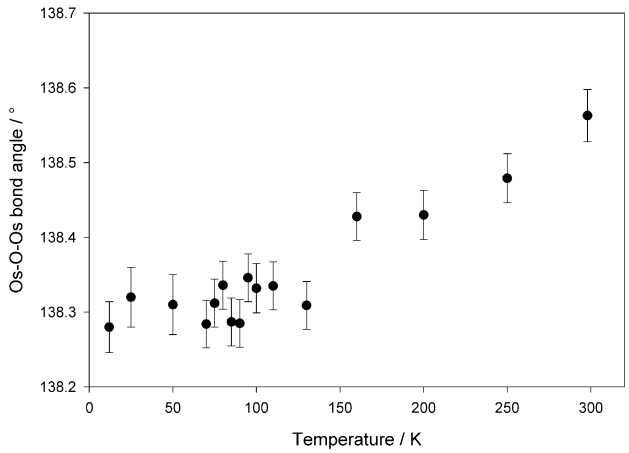

Fig. 9 The variation in the inter-octahedral angle Os–O–Os between 12 and 298 K.

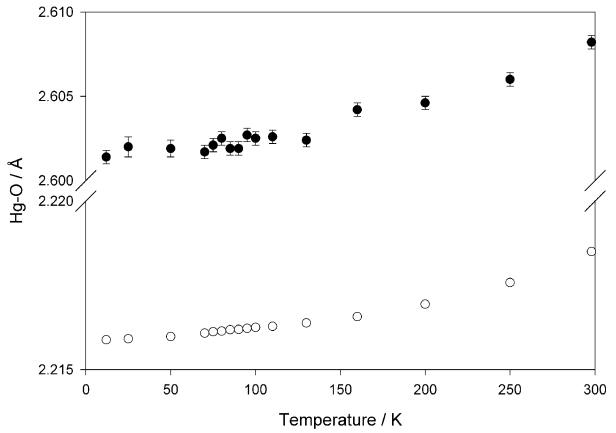

Fig. 10 The variation in the Hg–O bondlengths between 12 and 298 K.

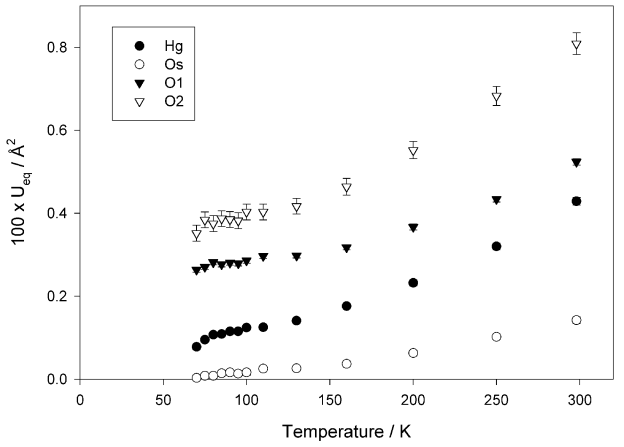

Fig. 11 Variations in the thermal displacement parameters measured from GEM data between 70 and 298 K.

apparent of a levelling off in each case between 80 and 100 K but the significance of this, in terms of the sizes of the esds on thermal displacement parameters, may not be high.

Conclusions and comparison with other 2+ 5+ pyrochlores

This structural, electronic and magnetic behaviour of $Hg_2Os_2O_7$ shows some similarities with that of $Cd_2Os_2O_7$ but in each case the magnitudes of any variations are far less marked. In terms of antiferromagnetic ordering this occurs at a much lower temperature, 88 K, than in the cadmium compound. As in the cadmium system anomalous behaviour in the Os–O distances for $Hg_2Os_2O_7$ is seen on approaching the transition temperature from below though, possibly because of the lower ordering temperature this variation is only weakly discernible. Neutron diffraction methods are required to observe these changes with any accuracy but the normal increase in metal–oxygen bond lengths on heating a material is not observed. This may be coupled with subtle changes in the electron distributions which seem to occur below about 100 K in $Hg_2Os_2O_7$. The non-appearance of magnetic reflections in the low temperature neutron diffraction data supports the view that the antiferromagnetic ordering is frustrated and has no long range order.

Clearly however there are marked differences in the electronic properties of these two osmate pyrochlore materials with $Hg_2Os_2O_7$ remaining semi-metallic down to 4 K in behaviour similar to that of $Cd_2Re_2O_7$ and $Cd_2Ru_2O_7$. The origin of these differences will require more detailed calculations on the band structure of $Hg_2Os_2O_7$. However Mandrus *et al*[9] note that the Cd states have a presence at the Fermi level of $Cd_2Os_2O_7$ (and the Tl states similarly in $Tl_2Mn_2O_7$) so that hybridisation between the osmium–oxygen and cadmium–oxygen levels is probably important in defining the electronic properties of this material. Hence replacement of cadmium by mercury can clearly be expected to modify the electronic behaviour quite markedly. An alternative explanation might lie in material non-stoichiometry as has been proposed for the difference between $Cd_2Re_2O_7$ and $Cd_2Os_2O_7$ with the former possibly being off-stoichiometry. However any such deviation must be small and no significant discrepancy in Hg site occupancy could be refined for $Hg_2Os_2O_7$ in this work.

Further structural studies of materials from these systems such as $Ca_2Os_2O_7$ and $Cd_2Os_2O_7$ are planned as well as more detailed investigation of the electronic and magnetic behaviour of $Hg_2Os_2O_7$.

Acknowledgement

We thank Prof. P. A. J. de Groot for access to the VSM and DERA for studentship support for J. R.

References

1 M. A. Subramanian, G. Aravamudan and G. V. Subba Rao, *Prog. Solid State Chem.*, 1983, **15**, 55.
2 B. J. Kennedy, *Physica B*, 1998, **241–243**, 303.
3 J. E. Greedan, J. N. Reimers, C. V. Stager and S. L. Penny, *Phys. Rev. B*, 1991, **43**, 5682.
4 B. D. Gaulin, J. S. Gardner, S. R. Dunsiger, Z. Tun, M. D. Lumsden, R. F. Kiefl, N. P. Raju, J. N. Reimers and J. E. Greedan, *Physica B*, 1998, **241**, 511.
5 Y. Shimakawa, Y. Kubo, T. Mnako, Y. V. Sushko, D. N. Argyriou and J. D. Jorgensen, *Phys. Rev. B*, 1997, **55**, 6399.
6 M. A. Subramanian, B. H. Toby, A. P. Ramirez, W. J. Marshall, A. W. Sleight and G. H. Kewi, *Science*, 1996, **273**, 81.
7 A. W. Sleight, J. L. Gillson, J. F. Weiher and W. Bindloss, *Solid State Commun.*, 1974, **14**, 357.
8 J. Reading and M. T. Weller, *J. Mater. Chem.*, 2001, **11**, 2373.
9 D. M. Mandrus, J. R. Thompson, R. Gaal, L. Forro, J. C. Bryan, C. C. Chakoumakos, L. M. Woods, B. C. Sales, R. S. Fisherman and V. Keppens, *Phys. Rev. B*, 2001, **6319**, 5104.
10 H. Sakai, K. Yoshimura, H. Ohno, T. D. Matsuda, H. Kato, S. Kambe, R. Walstedt, Y. Haga and Y. Onuki, *J. Phys.: Condens. Matter*, 2001, **13**, L785.
11 D. J. Singh, P. Blaha, K. Schwarz and J. O. Sofo, *J. Phys.: Condens. Matter*, in press.
12 R. F. Sarkozy and B. L. Chamberland, *Mater. Res. Bull.*, 1973, **8**, 1351.
13 B. Chamberlain, *Mater. Res. Bull.*, 1978, **13**, 1273.
14 I. S. Shalplygin and V. B. Lazarev, *Thermochim. Acta*, 1979, **33**, 53.
15 F. Abraham, J. Trehoux and D. Thomas, *J. Inorg. Nucl. Chem.*, 1980, **42**, 1627.
16 A. C. Larson and R. B. von Dreele, *Generalised Structure Analysis System*, Los Alamos National Laboratory, NM, 1994.
17 Special feature section, *Neutron News*, 1992, **3**, 29. Also available at http://www.ncnr.nist.gov/resources/n-lengths/
18 R. Wang and A. Sleight, *Mater. Res. Bull.*, 1998, **33**, 1005.